Systemic Targeting Inhibitor of κB Kinase Inhibits Melanoma Tumor Growth

Jinming Yang,[1] Wei-Hua Pan,[2] Gary A. Clawson,[2] and Ann Richmond[1]

[1]Department of Cancer Biology, Vanderbilt University School of Medicine and Veterans Affairs Medical Center, Nashville, Tennessee and [2]Department of Pathology, Department of Biochemistry and Molecular Biology, The Gittlen Cancer Research Institute, Hershey Medical Center, Pennsylvania State University, Hershey, Pennsylvania

Abstract

Constitutive activation of nuclear factor-κB (NF-κB) has been directly implicated in tumorigenesis of various cancer types, including melanoma. Inhibitor of κB kinase (IKK) functions as a major mediator of NF-κB activation. Thus, development of an IKK-specific inhibitor has been a high priority, although it remains unclear whether systemic inhibition of IKK will provide therapeutic benefit. In this study, we show that inhibition of NF-κB activity in melanocytes that are persistently expressing an active *H-Ras*^{V12} gene and are deficient in the tumor suppressors inhibitor A of cyclin-dependent kinase 4/alternative reading frame results in reduction of melanoma tumor growth *in vivo*. This effect is, at least in part, via regulation of NF-κB nuclear activation and RelA phosphorylation. Based on this result, we developed a double hammerhead ribozyme long-term expression system to silence either IKKα or IKKβ. The ribozymes were placed in an EBV construct and delivered i.v. to nude mice bearing melanoma lesions, which developed after i.v. injection of H-Ras–transformed melanoma cells. Our *in vivo* data show that knockdown of endogenous IKKβ significantly reduces the growth of the melanoma lesions and knockdown of either IKKα or IKKβ prolongs the life span of immunocompetent mice. [Cancer Res 2007;67(7):3127–34]

Introduction

The mammalian nuclear factor-κB (NF-κB) family contains five proteins, RelA/p65, NF-κB1 (p50), NF-κB2 (p52), c-Rel, and RelB, which can form a variety of homodimers and heterodimers to differently control gene expression. The NF-κB proteins share a Rel homology domain in the NH_2-terminal region that mediates dimerization, binding of DNA and/or inhibitor of NF-κB (IκB). NF-κB proteins are normally sequestered in the cytoplasm through interactions with IκB family of proteins (1). On activating signals, the IκB kinase (IKK) complex is activated by phosphorylation. The activated IKK subsequently phosphorylates IκB proteins followed with ubiquitination and degradation by 26S proteasome, thus allowing the NF-κB complex to translocate into the nucleus and bind to target DNA promoter sequences. NF-κB proteins were initially identified as pivotal transcription factors in chronic inflammatory diseases (2). Accumulating evidence indicates that NF-κB, as a central regulator of gene expression, plays a crucial role in controlling cell proliferation, apoptosis, and tumorigenesis (3–6). This is associated with constitutive IKK activity (7, 8). The IKK complex mainly comprises the catalytic subunits IKKα, IKKβ, and NF-κB essential modulator (NEMO) or IKKγ. Inhibition of IKK suppresses tumor cell growth, but the exact role of NF-κB in tumorigenesis may be dependent on tumor type (9). For example, it has been reported that NF-κB inhibition induces cancer in some mouse models (10, 11).

Increased understanding of the cell cycle pathways and genetic alterations involve in inhibitor A of cyclin-dependent kinase (CDK) 4/alternative reading frame (*INK4a/ARF*) gene. In some cases, the risk of developing melanoma runs in families, where a mutation in the *CDKN2A* gene on chromosome 9p21 can underlie susceptibility to melanoma (12, 13). *CDKN2A* encodes two distinct tumor suppressor proteins in alternative reading frames: the CDK inhibitor p16/INK4a and the p53 activator p14/ARF. Interestingly, the wild-type p16/INK4a binds to NF-κB/p65, whereas mutant p16/INK4a exhibits reduced binding activity and results in increased NF-κB activity (14). Moreover, p14/ARF functions as an IκB through activating p53 that in turn represses IKKα promoter activity, IKKα mRNA, and protein expression (15). Thus, loss/inactivation of the *INK4a/ARF* gene was postulated a contributor of the pathogenesis of melanoma in a NF-κB–dependent manner. However, in our mouse model, INK4a/ARF deficiency alone is not sufficient to induce melanoma (16). However, in cooperation with an active oncogene, such as H-ras, INK4a/ARF$^{-/-}$ melanocytes progress into melanoma (17).

The Ras proteins (H-ras, K-ras, and N-ras) regulate cell proliferation, survival, and differentiation. But specific point mutations in codon 12, 13, or 61 in one of the three Ras genes convert them into active oncogenes. Ras gene mutations have been found in a variety of tumor types (18). In agreement with this genetic alteration, a great many sporadic melanomas exhibit inactive INK4a, and melanocytes carrying germ-line deficiencies in the INK4a sequence exhibit a dramatically increased lifetime risk of melanoma (19). For decades, Ras proteins have been widely investigated. Ras cycles between the GDP-bound inactive form and the GTP-bound active form. The activated Ras activates two major pathways, Raf/mitogen-activated protein kinase/extracellular signal-regulated kinase (ERK) kinase (MEK)/ERK/activator protein-1 (AP-1) and phosphatidylinositol 3-kinase (PI3K)/Akt/NF-κB, both of which are greatly associated with carcinogenesis (20, 21). However, the mechanism for Ras activation of these pathways is unclear. For instance, in Ras-transformed melanocytes, B-Raf depletion did not block MEK-ERK signaling or cell cycle progression (22). Whether NF-κB plays a role in Ras transformation of melanocytes remains unclear.

Although a previously established mouse model confirms a causal role for H-Ras^{V12} with loss of INK4a/ARF in melanoma development (18), the interaction between H-Ras^{V12} oncogene

Note: Supplementary data for this article are available at Cancer Research Online (http://cancerres.aacrjournals.org/).

Requests for reprints: Ann Richmond, Department of Cancer Biology, Vanderbilt University School of Medicine, 771 PRB, 21st Avenue South at Pierce, Nashville, TN 37232. Phone: 615-343-7777; Fax: 615-936-2911; E-mail: ann.richmond@vanderbilt.edu.

doi:10.1158/0008-5472.CAN-06-3547

and NF-κB–mediated signals in melanocytes has not been fully characterized *in vivo*. Approaches for the study of NF-κB function *in vivo* often use transgenic or knockout animals. However, with NF-κB, this technique often produces lethality *in utero*, compromising examination of phenotypes in adult mice. To create a better understanding of the role of NF-κB in melanoma tumors, we developed a novel system that allows manipulation and monitoring of NF-κB activity with real-time *in vivo* imaging during H-Ras^{V12}–induced melanoma tumor growth. We also developed a novel systemic double ribozyme-based approach to specifically silence IKK in metastatic melanoma. Our results illustrate that NF-κB activity facilitates melanoma tumor growth and suggest that NF-κB is a potential therapeutic target for treatment of melanoma.

Materials and Methods

Construction of inducible retroviral vectors. To generate the retroviral Tet regulatory vector, pRevTet-On (Clontech, Palo Alto, CA) was inserted at the *Bam*H1 site with a transcription blocker that is composed of adjacent polyadenylation and transcription pause sites for reducing background transcription and a NF-κB consensus sequence fused to a TATA-like promoter and followed by a luciferase reporter gene for monitoring NF-κB signaling. This retroviral tetracycline transactivation vector was designated as Ta-NF-κB. To create the retroviral Tet response vector, pRevTre (Clontech) was inserted at the *Xho*1 site with a human cytomegalovirus (CMV) promoter to drive the expression of the constitutively active human *H-ras^{V12}* gene. To reduce leakiness of expression, the TRE containing seven direct repeats of the *tetO* operator sequence and an upstream minimal CMV promoter were replaced between the sites of *Bam*H1 and *Eco*R1 with a tight Tet-responsive promoter from the pTRE-Tight vector (Clontech). The Flag-IκBαAA was inserted into multiple cloning sites between *Eco*R1 and *Sph*1. This retroviral response vector was designated as Tr-Ras-IκB (Supplementary Fig. S1*A*).

Establishment of stable inducible cell lines. INK4a/ARF$^{-/-}$ murine melanocytes were infected with the retroviral vectors described above that were packaged in GP2-293 cells. A single colony expressing luciferase was selected and used as control cell line (designated C-melanocytes). The C-melanocytes were subsequently infected with the Tr-Ras-IκB retrovirus and then selected for 2 weeks in 500 μg/mL hygromycin (Sigma, St. Louis, MO) followed by limiting dilution selection of single colonies that persistently expressed the *H-Ras^{V12}* gene and inducibly expressed IκBαAA (Supplementary Fig. S1*B*). The emerging positive colony was designated as the Ras-melanocytes. The Ras-melanocytes formed melanoma tumors in nude mice, and the cells derived from the tumor were designated as Ras-melanoma cells.

Library selection of double hammerhead ribozymes. To identify the ribozyme targeting sites for IKKα and IKKβ, a library selection technique was used as described (23). After library selection, the double hammerhead ribozyme (dRz) sequence was identified and the specific cleavage sites in the IKK kinase domain were determined to be G131 and E232 for IKKα and V152 and L256 for IKKβ (as indicated in Fig. 3*A*). The "Rz core" refers to the ribozyme catalytic sequence (CTGATGAGTCCGTGAGGACGAAA). The SNIP$_{AA}$ cassette is a self-catalytic processing ribozyme cassette (Fig. 3*B* illustrates the schematic SNIP$_{AA}$ cassette in the *left* and its sequence in the *right*). The dRzIKK (Fig. 3*B, solid line*) was cloned into the SNIP$_{AA}$ cassette between *Bgl*II and *Mfe*I sites in the Clip portion and *Bam*HI and *Eco*RI sites in Chop portion. Self-processing, *cis*-acting ribozymes (Fig. 3*B, dashed line*) around the Clip and Chop portions function to liberate the dRzIKK. Finally, the SNIP$_{AA}$-dRzIKK was cloned into nonreplicating EBV-based plasmid (24, 25), designated as the p4486 vector, for long-term expression of the dRzIKK.

***In vivo* studies.** Animal experimentation was carried out according to protocols approved by the Institutional Animal Care and Use Committee/Department of Animal Care at Vanderbilt University. BALB/c-*nu/nu* female mice (10 mice per group) at age of 6 to 8 weeks were used. Injections of either plasmid or melanoma cells (2×10^5 to 4×10^5) were carried out via mouse tail vein in a final volume of 2 mL for each mouse body weight between 25 and 30 g. For *in vivo* induction of the tetracycline-responsive promoter that confers expression of Flag-IκBαAA, the mouse drinking water included doxycycline (1 mg/mL) and 5% sucrose, whereas the control group received only sucrose-enriched water. To examine intratumoral NF-κB activity, luciferin (150 μg/g body weight) was i.p. injected to each mouse 15 min before luminescent imaging using the IVIS 200 Imaging System (Xenogen Corp., Alameda, Ca). Photographs were taken and the luminescent intensity of each tumor was quantified to reflect the relative NF-κB activity *in vivo*.

Terminal deoxynucleotidyl transferase–mediated dUTP nick end labeling assay. The DeadEnd Fluorimetric [terminal deoxynucleotidyl transferase–mediated dUTP nick end labeling (TUNEL)] system from Promega Corp. (Madison, WI) was used to detect apoptosis by fluorescence-activated cell sorting analysis in the cultured melanoma cells and by staining of paraffin-embedded tumor tissues following the manufacturer's protocol.

Immunoprecipitation and kinase assay and Western blot analysis. Immunoprecipitation for IKKα/β proteins and IKK activity assays as well as the experimental protocol for Western blotting of these proteins were carried forth as we have previously described (7).

Reverse transcription-PCR. Total RNA was isolated from homogenized liver using Trizol (Invitrogen Life Technologies, Carlsbad, CA), and the first-strand cDNA was generated using Promega kit according to the manufacturers' protocols. The primers used in PCR were as follows: macrophage inflammatory protein-2 (MIP-2; 302 bp), TTCTCTGTGCAGCGCTGCTG (sense) and GACGGTGCCATCAGAGCAG (antisense); fibroblast growth factor 1 (FGF1; 415 bp), AGATCACAACCTTCGCAGCC (sense) and TTCTGGCCATAGTGAGTCCG (antisense); vascular endothelial growth factor (VEGF; 352 bp), ACTGCTGTACCTCCACCATGC (sense) and TTGGTCTGCATTCACATCTGC (antisense); hepatocyte growth factor (HGF; 408 bp), AACTCTGCAGATGAGTGTGCC (sense) and GACTTCGTAGCGTACCTCTGG (antisense); tumor necrosis factor α (TNFα; 305 bp), TGCCTATGTCTCAGCCTCTTC (sense) and GGCACCACTAGTTGGTTGTC (antisense); IFNγ (307 bp), TGCAGCTCTTCCTCATGGC (sense) and TGGATTCCGGCAACAGCTG (antisense); and glyceraldehyde-3-phosphate dehydrogenase (GAPDH; 249 bp), TGATGACATCAAGAAGGTGGTGAA (sense) and TCCTTGGAGGCCATGTAGGCCAT (antisense). The PCR products were resolved by electrophoresis in a 2% agarose gel and visualized by ethidium bromide staining.

Statistical analysis. Results are expressed as mean ± SD from two or three independent experiments. Statistical analyses used the unpaired Student's *t* test. $P < 0.05$ was considered statistically significant.

Results

NF-κB activation contributes to melanocyte transformation by oncogenic H-Ras^{V12}. To gain insight into the role of NF-κB in melanocyte transformation by oncogenic H-Ras^{V12}, we generated a retroviral Tet-inducible system in which a consensus sequence for the NF-κB promoter element was fused to a TATA-like promoter followed by a luciferase reporter gene. In cells expressing this reporter construct, it is possible to monitor NF-κB–regulated transcription and biological activity through real-time *in vivo* imaging of tumor development in response to expression of H-Ras^{V12} and loss of INK4a/ARF. Melanocytes were also transfected with a construct encoding the superrepressor of NF-κB, IκBα 32A/36A (IκBαAA), which is inducible with doxycycline (Supplementary Fig. S1*A* and *B*). In the presence of doxycycline, there is overexpression of this IκB mutant, which cannot be phosphorylated or degraded, thus keeping RelA/p50 in the cytoplasm. In comparison with control melanocytes not expressing H-ras^{V12} (Fig. 1*A, lane 1*), cellular NF-κB activity was induced 14.6 ± 3.2–fold

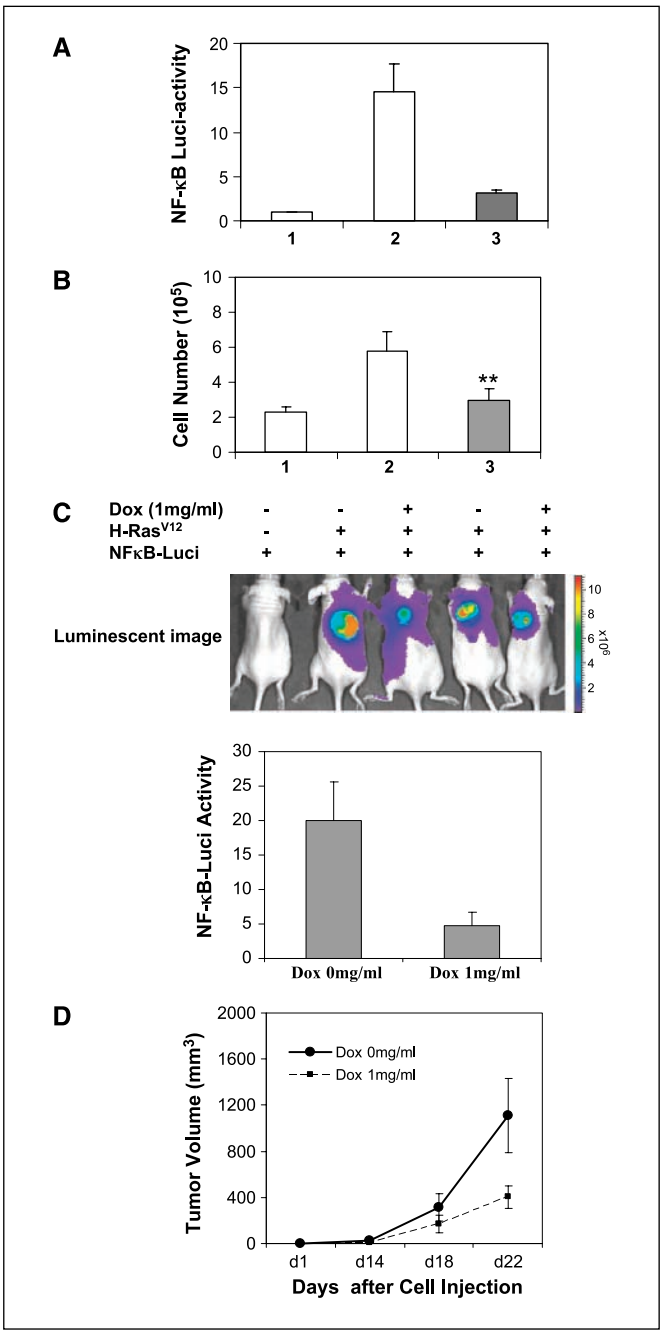

Figure 1. NF-κB activation is required for melanoma formation induced by H-Ras^{V12}. *A,* H-Ras^{V12} induction of NF-κB activity *in vitro*. Primary Ras-melanocytes stably expressing the *H-Ras^{V12}* gene (*lanes 2* and *3*) and inducibly expressing IκBαAA (*lane 3*) were cultured in medium containing (*solid box*) or not containing (*open box*) 1 μg/mL doxycycline for 48 h. *Lane 1,* the C-melanocytes not expressing H-Ras^{V12} were used as a negative control. The cell lysate was subjected to luciferase activity assay. *B,* cell proliferation assay *in vitro*. The C-melanocytes not expressing H-Ras^{V12} (*lane 1*) and the H-Ras^{V12}–transformed melanocytes (*lanes 2* and *3*) were cultured in the absence (*white column*) or presence (*black column*) of 1 μg/mL doxycycline for 5 d. The cell number was counted and analyzed statistically. Data were from two duplicate experiments. *C,* real-time *in vivo* imaging of NF-κB activity. Mice were inoculated with C-melanocytes or Ras-melanocytes; simultaneously, mice were treated or not treated with doxycycline (*Dox*) in the drinking water to induce IκBαAA expression. At the end of experiment, mice (n = 10) were injected i.p. with 0.15 mg luciferin per gram body weight and subjected to luminescent imaging (*top*) and quantified for the relative NF-κB-luciferase reporter activity (*bottom*). *D,* measurement of tumor size. Tumor size was measured using a digital caliper and volume was calculated as described in Materials and Methods. The entire experiment was repeated and similar results were obtained.

by H-ras^{V12} (Fig. 1*C, lane 2*), and this induction was significantly blunted (to 3.2 ± 0.33–fold) by doxycycline induction of IκBαAA expression (Fig. 1*A, lane 3*). In agreement with cellular NF-κB activity, the cell proliferation of the H-Ras^{V12}–transformed melanocytes exhibited a 2.5-fold increase (Fig. 1*B, lane 2*) compared with melanocytes not expressing H-ras^{V12} (Fig. 1*B, lane 1*). However, the H-Ras^{V12}–enhanced cell proliferation was inhibited 48% when doxycycline was added to the culture medium to induce IκBαAA expression (Fig. 1*B, lane 3*). To examine the relationship between H-Ras^{V12} induction of NF-κB–mediated transcription and tumor growth, INK4a/ARF$^{-/-}$ melanocytes containing an integrated retroviral inducible vector system (Ras-melanocytes) were inoculated s.c. into nude mice and 1 mg/mL doxycycline was simultaneously added (or not added) to the drinking water. Intratumoral NF-κB activity was estimated by quantitative luminescent imaging over a time frame of 22 days (Fig. 1*C*). The relative NF-κB reporter activity in tumors in mice without doxycycline treatment was 20 ± 4.8, whereas only 4.8 ± 1.9 NF-κB activity was observed in the tumors of mice with doxycycline treatment, indicating a 76% inhibition of NF-κB reporter activity (n = 10; P < 0.01; Fig. 1*C*). After 22 days, tumor volume reached 1,110 ± 320 mm^3 without doxycycline treatment but was only 405 ± 98 mm^3 when mice received doxycycline, indicating a 63% inhibition of tumor growth (n = 10; P < 0.01; Fig. 1*D*). Mice injected with INK4a/ARF$^{-/-}$ mouse melanocytes stably expressing the NF-κB-luciferase reporter (C-melanocytes) failed to develop tumors (Fig. 1*C, lane 1*). These results show that H-Ras^{V12}–induced melanocyte transformation is partially, if not fully, via activation of the NF-κB pathway.

IKK complex is activated by H-Ras^{V12} and triggers NF-κB activation. To elucidate the biochemical mechanism of the H-Ras^{V12}–induced NF-κB activation, IKKα/β were immunoprecipitated from cells with or without H-Ras^{V12} expression and *in vitro* kinase assays were done using RelA as a substrate (26). Cells stably expressing H-Ras^{V12} (Fig. 2*A, lane 2*) exhibited enhanced IKK activity, indicating that H-Ras^{V12}–induced NF-κB activity was through IKKα/β activation. To extend this finding, cell lysates were subjected to Western blot to assess IκBα protein expression and IκBα phosphorylation. Data (Fig. 2*B*) indicate that increased phosphorylation of IκBα (Fig. 2*B, top, lane 2*) occurs in response to H-Ras^{V12}–induced IKK activity. Moreover, the overexpression of the superrepressor mutant of IκB, IκBαAA, by addition of doxycycline to the culture medium, abrogates the endogenous IκBα phosphorylation induced by expression of H-Ras^{V12}.

Because phosphorylation of RelA is also important for optimal NF-κB–mediated transcription, we examined whether RelA phosphorylation is involved in H-Ras^{V12}–induced NF-κB activation. Data show that melanocytes expressing H-Ras^{V12} exhibited persistent RelA phosphorylation (Fig. 2*C*, *lane 2* versus control in *lane 1*), which was subsequently diminished to the basal level by expression of IκBαAA (Fig. 2*C, lane 3*). To further obtain biochemical evidence of IκBαAA blockage of the phosphorylation of RelA, we reconstituted a cell-free system in which immunoprecipitated IKKα/β (Fig. 2*D, bottom*), purified glutathione *S*-transferase (GST)-IκBαAA, GST-RelA, and [γ-^{32}P]ATP were incubated at 30°C for 30 min. The results revealed that IκBαAA blockage of RelA phosphorylation was through competition for IKK activity because increasing amounts of GST-IκBαAA diminished the RelA phosphorylation.

Cumulative data show that mutant Ras-activated Raf/MEK/ERK and PI3K/AKT pathways contribute to the melanoma

transformation (20). To clarify whether inhibition of NF-κB affects the above signal proteins, we treated H-Ras^{V12}–transformed melanoma cells with 1 μg/mL doxycycline for 14 h and then examined the phosphorylation status of cellular ERK and AKT. The results showed that the H-Ras^{V12}–elevated phosphorylation levels of both ERK and AKT were not altered by IκBαAA expression (data not shown). Therefore, IκBαAA targets the specific NF-κB complex downstream of PI3K/AKT but not the ERK/AP-1 pathway.

Development of dRz reagent and long-term specific silencing of the IKK in melanoma metastatic site in adult mice. Although constitutive IKK activity is associated with NF-κB activation in various cancers (27, 28), including human melanoma (29), whether IKKα or IKKβ is able to serve as a therapeutic target for melanoma is still not established. IKKβ is far more potent than IKKα in phosphorylating IκBα. Studies into the function of IKK in tumorigenesis have been difficult using either IKKα/β knockout animals or by an antisense oligonucleotide-based gene knockdown approach because the former method interferes with embryonic development (30, 31), whereas the latter has poor efficiency (32). To achieve an approach that stably and specifically disrupts the *IKK* gene in adult animals, we developed a dRz system using library selection technology to optimize specific target sites (2) within the IKK kinase domain (Fig. 3*A*). The dRzIKKα targets mRNA sequences surrounding sites of 393G and 693G, corresponding to amino acid glycine (G) 131 and glutamic acid (E) 232 within the IKKα protein. The dRzIKKβ targets sequences surrounding mRNA sites of 465C and 793C, corresponding to amino acid valine (V) 152 and leucine (L) 265 within the IKKβ protein. The dRzIKK (Fig. 3*A, solid line*) was cloned into the SNIP$_{AA}$ cassette within Clip and Chop portion, respectively. Either the Clip or Chop portion is located between self-processing, *cis*-acting ribozymes (Fig. 3*A, dash line*). In this instance, the anti-IKKα (or IKKβ) SNIP$_{AA}$-dRz is able to target two optimally accessible mRNA sites within the mRNA (one dRz is released from the Clip portion and another from the Chop portion). For systemic delivery of dRzIKK to tumor-bearing mice with long-term expression without evoking an antiviral response, the SNIP$_{AA}$ containing either dRzIKKα or dRzIKKβ was cloned into nonreplicating EBV-based plasmid (24, 25), p4486 vector. To evaluate the efficiency of dRz to knock down the IKK target, dRzIKK and/or Flag-IKK vector DNA were cotransfected into 293T cells, and the expression of the Flag-tagged IKK protein was analyzed by Western blotting with anti-Flag antibody. ERK2 protein was blotted as a control to monitor equal loading. Results showed that either the dRzIKKα or the dRzIKKβ was able to significantly knock down its target protein expression in contrast to the dRzUGT control (Fig. 3*C*). UGT is an IKK-unrelated enzyme (UDP-glucuronosyltransferase) that is responsible for metabolic inactivation of estrogens in breast tissue. To test the potential of the p4486 vector for reporting dRz expression, a luciferase reporter gene was cloned into the vector. After 100 μg vector DNA was injected i.v. into the mouse, luciferase activity was followed by luminescent imaging and quantified (Supplementary Fig. S2*A*). Vector-mediated luciferase expression was explored *in vivo* for 60 days after a single injection. Addition of the 3′-polyadenylic acid [3′-poly(A)] tail to the optimal dRz selected from the library enhanced the stability of the liberated dRz (Fig. 3*B, right*) and contributed to the long-term silencing of IKK genes. To validate the dRz silencing of IKK *in vivo*, 100 μg of dRzIKK in p4486 vector DNA were packaged using the TransIT *In Vivo* Gene Delivery System (Mirus, Madison, WI) and delivered via mouse tail i.v. injection. The protein expression of either IKKα or IKKβ in liver was determined by Western blot. Data (Fig. 3*D*) show that the dRzIKK approach efficiently silenced IKKα and IKKβ gene expression with prolonged duration (40 days) after a single dosage application. We showed that either dRzIKKα or dRzIKKβ effectively silenced target gene expression *in vitro* and *in vivo*.

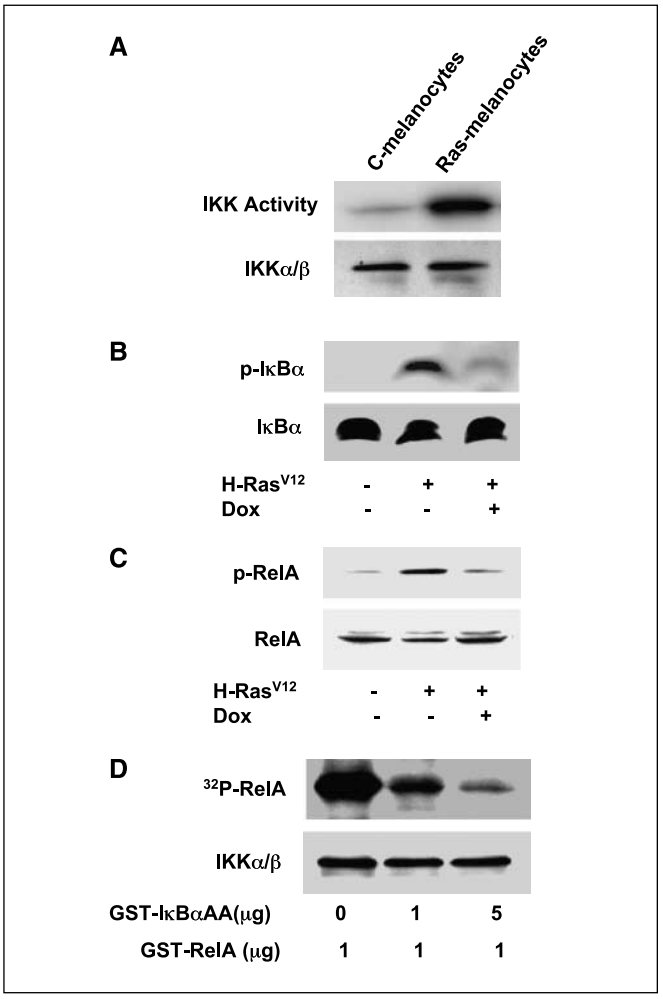

Figure 2. H-Ras^{V12} regulates NF-κB signaling. *A,* H-Ras^{V12} induction of IKK phosphorylation. C-melanocytes (not expressing H-ras^{V12} protein) or Ras-melanocytes (expressing H-ras^{V12} protein) were lysed and immunoprecipitated with IKKα/β antibodies. The immunocomplex was incubated with the IKK substrate, GST-RelA, and [γ-^{32}P]ATP, and IKK activity was visualized by PAGE and autoradiography. The IKKα/β proteins were immunoblotted with the same antibodies described elsewhere (9). *B,* IκBαAA inhibition of endogenous IκBα phosphorylation. C-melanocytes or Ras-melanocytes were cultured in the absence or presence of doxycycline. Western blot analysis was done for cytosolic (unphosphorylated) or phosphorylated IκBα (*p-IκBα*) with specific antibodies. *C,* IκBαAA inhibition of endogenous RelA phosphorylation was evaluated by Western blot. *D,* IκBαAA competitively inhibits RelA phosphorylation. A cell-free system was constituted by immunoprecipitation of IKK from human SK-Mel-5 cells, which was incubated with the substrate GST-RelA, GST-IκBαAA, as indicated, and [γ-^{32}P]ATP. The [γ-^{32}P]-labeled RelA protein was then visualized by PAGE and autoradiography (9).

dRz knockdown of IKK in melanoma metastatic host organ slows tumor growth and prolongs life span in immunocompetent mice. To evaluate the targeting tissue of metastatic melanoma, Ras-melanoma cells isolated from tumor xenograft

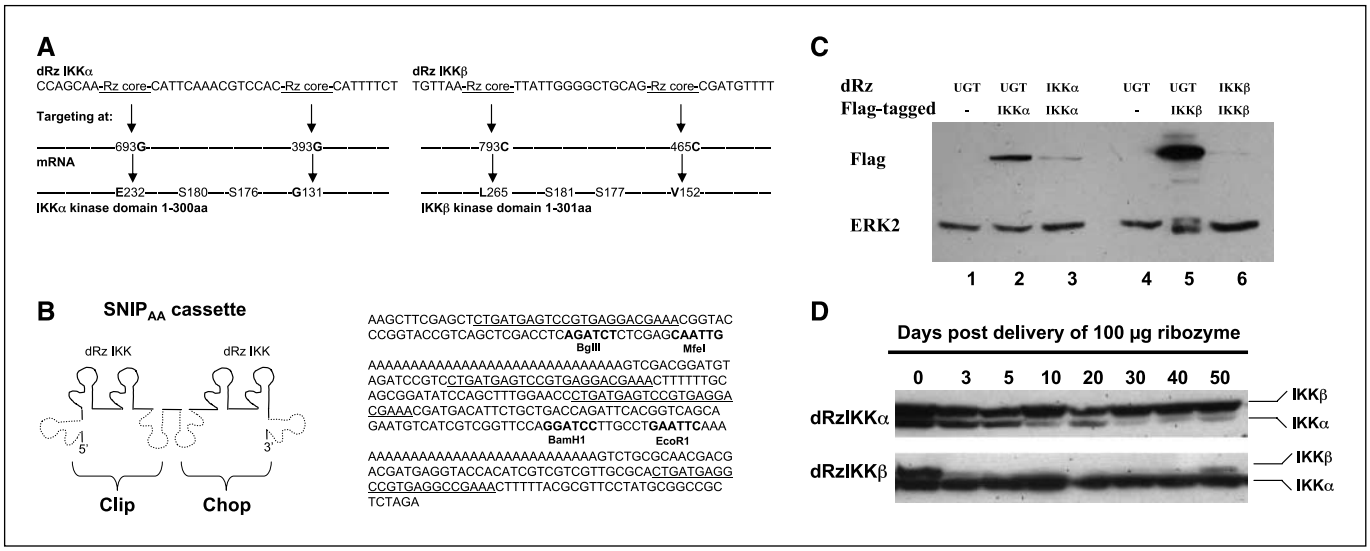

Figure 3. Characteristics of dRzIKK targeting of IKK and melanoma metastasis model. *A,* library selection of dRz targeting sites of IKKα (*left*) or IKKβ (*right*) within the IKK kinase domain. *B,* the SNIP$_{AA}$ cassette contains the dRzIKKs (*left*) and SNIP$_{AA}$ sequence (*right*). The dRzIKKs were inserted into both Clip (between the *Bgl*II/*Mfe*I site) and Chop (between *Bam*HI/*Eco*RI site). *C,* dRz constructs targeting either IKKα (dRzIKKα) or IKKβ (dRzIKKβ) efficiently reduced protein expression of the Flag-tagged target gene *IKKα* (*lane 3*) or *IKKβ* (*lane 6*), which was cotransfected into cultured 293T cells. Western blot of Flag-tagged IKK and ERK2 is included as loading controls. *D,* liver proteins were prepared at various times and the expression of IKKα or IKKβ was examined by Western blot analyses. Either IKKα or IKKβ was persistently reduced (by >90%) for 40 to 50 d after i.v. delivery of a single dose of 100 μg dRzIKK vector DNA.

were injected i.v. into BALB/c nude mice or C57/BL6 immunocompetent mice. Liver and lung were the main sites for melanoma metastases as revealed by luminescent imaging 2 months after injection of cells (Supplementary Fig. S2*B, left, inset*) and histologic analysis of H&E-stained liver sections (H&E staining of *left*). Ras-melanoma cells were also genetically engineered to express green fluorescent protein (GFP) and injected i.v. into nude mice. One month after injection, the frozen tissue sections from mouse organs were examined by fluorescence microscopy. The GFP-expressing melanoma cells were mainly localized in the liver (Supplementary Fig. S2*B, right*) in contrast to other organs, such as lung and kidney (data not shown). Coincidently, the liver also favored expression of the p4486-luciferase vector (Supplementary Fig. S2*A*).

To assess the overall role of IKKα or IKKβ in the metastatic melanoma and in the regulation of apoptosis, angiogenesis, and tumor progression, DNA constructs encoding the dRz (100 μg/mouse) were given i.v. monthly using the TransIT *In Vivo* Gene Delivery System beginning 3 days after tail vein injection of Ras-melanoma cells into nude mice. Eighty days after cell injection, the effects of expression of the dRzIKKα and dRzIKKβ on tumor NF-κB activity and tumor phenotype were examined. Data (Fig. 4*A* and *B*) indicate that the dRzIKK reduction in NF-κB activity was associated with slower tumor growth. Although the dRzIKKα caused a 53% reduction of tumor NF-κB activity, which coincided with a 13% reduction of tumor size, dRzIKKβ reduced NF-κB activity by 69% and reduced tumor growth by 40% ($P < 0.01$). To examine the direct effect of the cellular IKK knockdown on cell proliferation, the H-Ras^{V12}–transformed melanoma cells were transfected with a dRzIKK vector DNA and cultured for 5 days. In comparison with the cells transfected with the control dRzUGT, the cell proliferation was inhibited by 18.8% or 39.6% in the cells transfected with the dRzIKKα or dRzIKKβ (Fig. 4*C*). To determine whether knockdown of endogenous IKK is able to benefit tumor-bearing immunocompetent mice, Ras-melanoma cells were i.v. injected into each C57/BL6 mouse and mice were treated with dRzIKKα, dRzIKKβ, or dRzUGT by i.v. injection and observed for duration of 110 days. Knockdown of either dRzIKKα or dRzIKKβ markedly improved the survival in the melanoma-bearing animals by 6- and 7-fold, respectively, compared with the control mice treated with dRzUGT (Fig. 4*D*).

Melanoma cells with IKK knockdown are susceptible to cell death. To explore the role of dRzIKK antimelanoma activity, Ras-melanoma cells were injected i.v. into *nu/nu* nude mice. Three days after delivery of tumor cells, either dRzIKKα, dRzIKKβ, or dRzUGT (100 μg/mouse, monthly) was injected i.v. into mice (10 mice per group). Eighty days after tumor cell injection, mice were euthanized and liver tissues with the micrometastasis of Ras-melanoma cells were examined for apoptosis using TUNEL assay. Interestingly, apoptotic cells appeared in melanoma metastatic sections (Fig. 5*A*) when these mice were treated with either dRzIKKα or dRzIKKβ. However, we failed to observe apoptotic hepatocytes in the liver tissues from mice with the same treatment. Tumor sections from mice treated with dRzUGT rarely showed apoptotic cells. To examine whether dRzIKK directly affects melanoma cells, Ras-melanoma cells were transiently transfected with the dRzIKKα, the dRzIKKβ, or the dRzUGT p4486 vector *in vitro*. The subsequent TUNEL assay showed that the dRzIKKβ significantly induced apoptosis in melanoma cells ($P < 0.05$). Thus, the dRzIKKβ-mediated antitumor activity is through an apoptosis-dependent mechanism.

Angiogenesis is important for continuous growth of melanoma and other solid tumors. To gain insight into the effect of suppression of NF-κB on tumor angiogenesis, Ras-melanoma cells and dRzIKK were i.v. injected into mice. The mRNA profile of angiogenesis factors in melanoma lesions arising in the liver was examined using reverse transcription-PCR (RT-PCR) approach. As shown in Fig. 5*C*, inhibition of mRNA expression of angiogenesis-related genes, such as *MIP-2, FGF1, VEGF*, and *HGF*,

was indicated by knockdown of either IKKα or IKKβ. Thus, IKK plays crucial role in hepatic angiogenesis and melanoma tumor growth.

Discussion

The Ras proteins regulate cell proliferation, survival, and differentiation. A specific point mutation in codon 12 converts the *H-Ras* gene into an active oncogene. Ras gene mutations (H-Ras and N-Ras) have been found in a variety of tumor types, particularly in melanoma (18). However, Ras activation in melanocytes is not sufficient to induce melanoma unless the melanoma susceptibility gene *INK4a/ARF* is lost (17). In agreement with this genetic alteration, the majority of sporadic melanomas exhibit inactive INK4a, and melanocytes carrying germ-line deficiencies in the INK4a exhibit a dramatically increased lifetime risk of melanoma (19). Mutant Ras activates the Raf/MEK/ERK/AP-1 pathway, which was associated with carcinogenesis. However, the mechanism for Ras activation of this pathway is unclear. For instance, in Ras-transformed melanocytes, B-Raf depletion did not block MEK-ERK signaling or cell cycle progression (33). We questioned whether NF-κB is involved in Ras-transformed melanocytes. In this study, we focused on inhibition of NF-κB in H-Ras–induced melanocyte transformation. We generated a retroviral Tet-inducible system that provides a NF-κB reporter "window" into the organism and tracks the biological activities of H-Ras^{V12} and effects of expression of the IκB superrepressor (IκBαAA) during the pathogenesis of melanoma. Based on our results, H-Ras^{V12} melanoma tumor growth requires activation of the NF-κB pathway. Inhibition of NF-κB by IκBαAA in melanocytes decreases H-Ras^{V12}–induced melanoma growth. The tumor suppressor INK4a/ARF not only functions as a CDK inhibitor that leads to cell cycle arrest in the G_1 phase (34) but also directly interacts with RelA to inhibit NF-κB transcriptional activity (14). Thus, NF-κB activity in melanocytes with INK4a/ARF deficiency is easily induced by expression of H-Ras^{V12}. Given the important role that NF-κB plays in promoting melanoma tumor growth, it is not surprising that NF-κB activation is a key component in inflammation-based cancer progression (35).

Our investigation of the biomedical mechanism of the H-Ras^{V12}–induced NF-κB activation reveals that H-Ras^{V12} induces IKK activity, triggering the phosphorylation of IκBα and RelA. With induction of the expression of IκBαAA superrepressor, the phosphorylation of these two proteins is reduced to a basal level, resulting in inhibition of NF-κB transcriptional activity *in vitro* and *in vivo*. Numerous reports show that NF-κB is constitutively activated, as measured by either electrophoretic mobility shift assay or NF-κB-luciferase reporter assay, in a variety of tumor cells, including melanoma cells. In previous work from our laboratory, a kinetic study of RelA shuttling between the cytoplasm and the nucleus indicates that inhibition of the constitutive IKK activity blocks RelA nuclear translocation in human melanoma cells (9). In agreement with the previously described murine fibroblast model (36), the study here with a melanocyte model indicates that RelA is required for efficient cellular transformation induced by oncogenic H-Ras^{V12}. Extensive studies show that NF-κB activation promotes

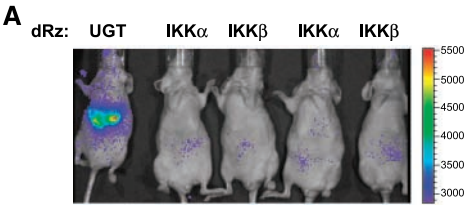

Double ribozyme	UGT	IKKα	IKKβ
NF-κB Activity	100%	47±12%	31±8%

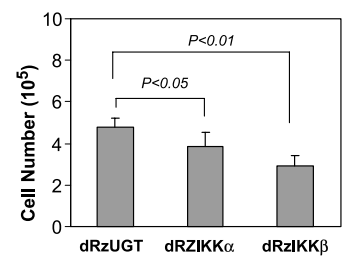

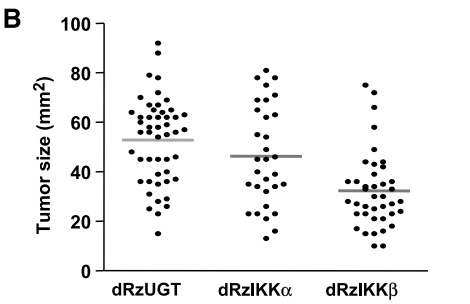

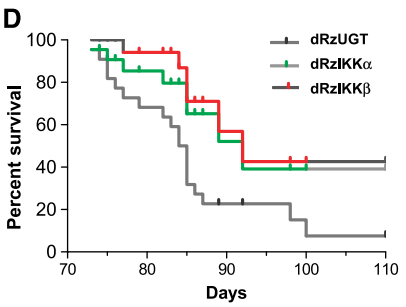

Double ribozyme	UGT	IKKα	IKKβ
Tumor size	53 ±17	46 ±20	32 ±15*
Tumor No.	49	31	40

* p<0.01, data from tumor-bearing nude mice (n=9), 200 fields of microscope

dRz	UGT	IKKα	IKKβ
Survival	2	12	14
Death	18	8	6
P value		<0.01	< 0.01

Figure 4. Antimelanoma activity of dRzIKK. *A,* dRzIKK reduction of NF-κB activity in the hepatic melanomas. Ras-melanoma cells (2×10^5) were injected i.v. into BALB/c-*nu/nu* female mice ($n = 10$/group). These mice were given dRz vector DNA (100 μg/mouse) i.v. every 30 d. Eighty days after injection of cells, mice were subjected to luminescent imaging (*A*) for the quantitative intratumor NF-κB activity and histologic analysis and (*B*) for the tumor size and number in liver sections containing melanoma micrometastases using the Image-Pro Plus program. *C,* knockdown of IKK inhibits cell proliferation. Ras-melanoma cells (2×10^5) were transfected with dRzUGT, dRzIKKα, or dRzIKKβ and cultured *in vitro*. Five days after culture, cell number was determined by hemocytometer counting and analyzed statistically. Data were from two triplicate experiments. *D,* dRzIKK prolongs the life span of melanoma-bearing mice. Ras-melanoma cells (5×10^5) were i.v. injected into C57/BL6 mice (20 mice/group) and dRzIKKα, dRzIKKβ, or dRzUGT was delivered by i.v. injection of 100 μg vector DNA monthly. The animal survival rate was scored for duration of 110 d. Data were plotted and analyzed using the GraphPad Prism program.

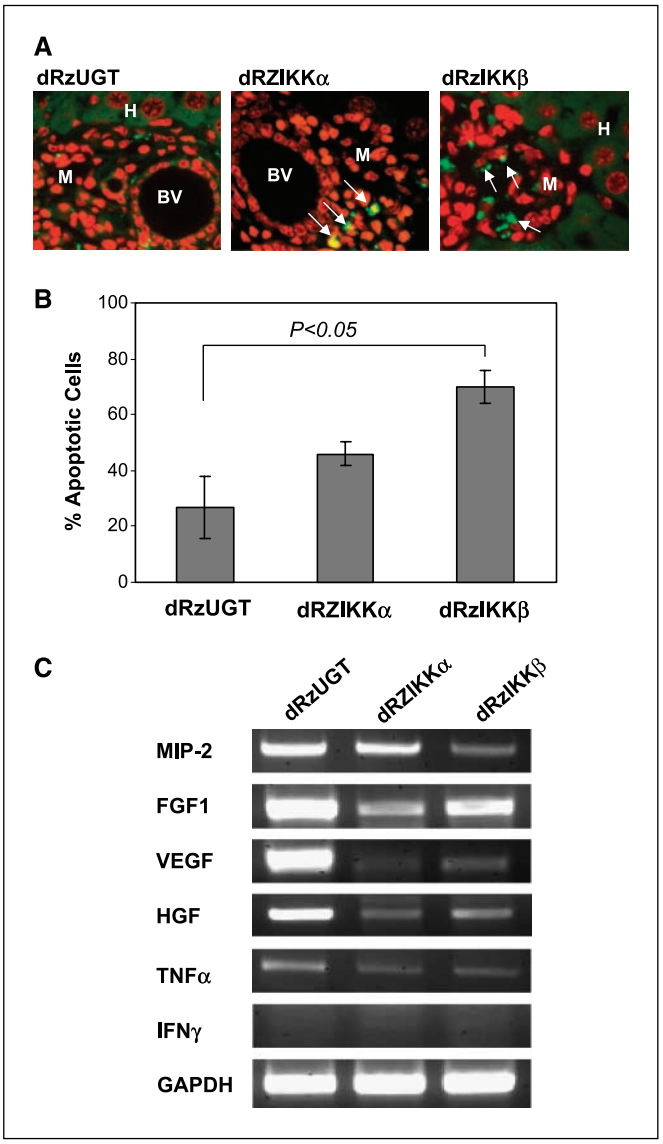

Figure 5. dRzIKK induction of cellular apoptosis. *A,* paraffin-embedded liver tissues with micrometastatic Ras-melanoma were subjected to DeadEnd Fluorometric TUNEL assay for detection of apoptosis. The TUNEL-positive cells are visualized in green fluorescence (*arrow*) in a red propidium iodide background by fluorescence microscopy. Data are from one of two independent experiments showing similar results. *BV,* blood vessel; *M,* melanoma cells; *H,* hepatocytes. *B,* Ras-melanoma cells (5×10^6) were transfected with either dRzIKKα, dRzIKKβ, or dRzUGT. Thirty-six hours after transfection, the apoptotic cells were examined using TUNEL assay and analyzed by flow cytometry by measuring fluorescein-12-dUTP at 520 nm. *C,* dRzIKK regulated expression of angiogenesis factors. Ras-melanoma cells (5×10^5) were i.v. injected into C57/BL6 mice (three mice/group) for 3 days, and subsequently, 100 μg vector DNA of dRzIKKα, dRzIKKβ, or dRzUGT was delivered i.v. Three days after dRzIKK injection, mice were euthanized and the livers were homogenized. The total RNA was extracted and subjected to RT-PCR assay for MIP-2, FGF1, VEGF, HGF, TNFα, and IFNγ. GAPDH was used as a loading control.

cell survival through induction of expression of antiapoptotic target genes. However, inhibition of NF-κB in keratinocytes facilitates epidermal cancer formation. For example, inhibition of NF-κB in murine epidermis by expression of IκBαAA using the epidermis-specific keratin 5 promoter results in inflammation, hyperplasia, and rapid development of squamous cell carcinoma (SCC; ref. 37). Additionally, when fetal skin deficient for RelA was transplanted into nude mice, the $RelA^{-/-}$ grafts develop keratinocyte hyperplasia and eventually SCC (38). One explanation for this phenomenon is that NF-κB function is cell type specific: in keratinocytes NF-κB is antitumorigenic and in melanocytes it is protumorigenic. In melanoma, breast cancer, and many other tumor types (7, 39), increased IKK activity results in enhanced RelA activation. The resultant cell survival advantage is a common mechanism for developing resistance to chemotherapy (40, 41).

Development of an IKK-specific inhibitor has been a high priority in pharmaceutical industries. Several candidate small-molecular inhibitors targeting IKK are currently under preclinical investigation (9, 40). Side effects from the treatment with IKK inhibitors are inevitable (42). The most important issue is whether systemic inhibition of IKK will provide therapeutic benefit. In this study, we developed a dRz long-term expression system to silence either IKKα or IKKβ. The dRzs were cloned into a $SNIP_{AA}$ cassette. The $SNIP_{AA}$-dRz cassette was shown to self-process efficiently *in vitro* and *in vivo* while providing significant advantages (43): (*a*) library selection of optimal target sites, (*b*) liberation of the targeted dRz with minimal nonspecific flanking sequences, (*c*) a designed 3′-poly(A) tail enhancing the stability of the liberated dRz, and (*d*) dRz distribution in both nucleus and cytoplasm. For systemic delivery of $SNIP_{AA}$-dRz cassette to tumor-bearing mice with long-term expression without evoking an antiviral response, a nonreplicating EBV-based vector (25) was used to express the $SNIP_{AA}$ cassette containing either dRzIKKα or dRzIKKβ. In this melanoma model, liver is the major site for metastasis, thus offering advantage for the vector-based ribozyme delivery, which is concentrated in the liver. Both dRzIKKα and dRzIKKβ were individually able to efficiently silence target gene expression in mice treated with either of these ribozymes. Knockdown of IKKβ, however, accounts for a significant reduction of the size of melanoma micrometastasis ($P < 0.01$). In agreement with this finding, recent investigations directly implicate that IKKβ is a key component in inflammation-based cancer progression (5, 44).

Conditional deletion of IKKβ in intestinal epithelium reduces tumor number but not tumor size, whereas deletion of IKKβ in myeloid cells reduces tumor size but not tumor number (35). In our study, importantly, systemic delivery of either dRzIKKα or dRzIKKβ reduces size of tumors and tumor burden and significantly prolongs the life span in melanoma-bearing immunocompetent adult mice. Tumor-host interaction is critical for melanoma growth and metastasis, and tumor angiogenesis plays a vital role in these events. Our data indicate that systemic silencing of IKK provides direct effects on $H\text{-}Ras^{V12}$– induced melanoma cell proliferation and angiogenesis, contributing to suppression of metastatic melanoma tumor growth.

In conclusion, our results clearly indicate an important role for NF-κB in $H\text{-}Ras^{V12}$–induced melanocyte transformation and imply that this pathway constitutes a reasonable therapeutic target for treatment of malignant melanoma.

Acknowledgments

Received 9/27/2006; revised 1/2/2007; accepted 1/29/2007.

Grant support: Department of Veterans Affairs Career Scientist Award (A. Richmond), CA56704 and CA116021 (A. Richmond), NIH-sponsored Vanderbilt-Ingram Cancer Center grant CA68485, and Skin Disease Research Center grant 5P30 AR41943.

The costs of publication of this article were defrayed in part by the payment of page charges. This article must therefore be hereby marked *advertisement* in accordance with 18 U.S.C. Section 1734 solely to indicate this fact.

We thank Robert J. Debs for providing the EBV-based vector p4486; Peng Liang for the $H\text{-}ras^{V12}$ expression vector; Linda W. Horton, Yinchun Yu, Ping Xin, and Snjezana Zaja-Milatoric for excellent technical assistance; and the Vanderbilt Editor Club for critical reading of the manuscript.

References

1. Ghosh S, Karin M. Missing pieces in the NF-κB puzzle. Cell 2002;109 Suppl:S81–96.
2. Coussens LM, Werb Z. Inflammatory cells and cancer: think different! J Exp Med 2001;193:F23–6.
3. Coussens LM, Werb Z. Inflammation and cancer. Nature 2002;420:860–7.
4. Balkwill F, Coussens LM. Cancer: an inflammatory link. Nature 2004;431:405–6.
5. Karin M, Greten FR. NF-κB: linking inflammation and immunity to cancer development and progression. Nat Rev Immunol 2005;5:749–59.
6. Gomperts BN, Strieter RM. Chemokine-directed metastasis. Contrib Microbiol 2006;13:170–90.
7. Yang J, Richmond A. Constitutive IκB kinase activity correlates with nuclear factor-κB activation in human melanoma cells. Cancer Res 2001;61:4901–9.
8. Baldwin AS. Control of oncogenesis and cancer therapy resistance by the transcription factor NF-κB. J Clin Invest 2001;107:241–6.
9. Yang J, Amiri KI, Burke JR, Schmid JA, Richmond A. BMS-345541 targets inhibitor of κB kinase and induces apoptosis in melanoma: involvement of nuclear factor κB and mitochondria pathways. Clin Cancer Res 2006;12:950–60.
10. Karin M. Nuclear factor-κB in cancer development and progression. Nature 2006;441:431–6.
11. Sakurai T, Maeda S, Chang L, Karin M. Loss of hepatic NF-κB activity enhances chemical hepatocarcinogenesis through sustained c-Jun N-terminal kinase 1 activation. Proc Natl Acad Sci U S A 2006;103:10544–51.
12. Hussussian CJ, Struewing JP, Goldstein AM, et al. Germline p16 mutations in familial melanoma. Nat Genet 1994;8:15–21.
13. Rizos H, Darmanian AP, Holland EA, Mann GJ, Kefford RF. Mutations in the INK4a/ARF melanoma susceptibility locus functionally impair p14ARF. J Biol Chem 2001;276:41424–34.
14. Becker TM, Rizos H, de la Pena A, et al. Impaired inhibition of NF-κB activity by melanoma-associated p16INK4a mutations. Biochem Biophys Res Commun 2005;332:873–9.
15. Gu L, Zhu N, Findley HW, Woods WG, Zhou M. Identification and characterization of the IKKα promoter: positive and negative regulation by ETS-1 and p53, respectively. J Biol Chem 2004;279:52141–9.
16. Yang J, Luan J, Yu Y, et al. Induction of melanoma in murine macrophage inflammatory protein 2 transgenic mice heterozygous for inhibitor of kinase/alternate reading frame. Cancer Res 2001;61:8150–7.
17. Chin L, Pomerantz J, Polsky D, et al. Cooperative effects of INK4a and Ras in melanoma susceptibility *in vivo*. Genes Dev 1997;11:2822–34.
18. Chin L, Tam A, Pomerantz J, et al. Essential role for oncogenic Ras in tumour maintenance. Nature 1999;400:468–72.
19. Mercurio F, Zhu H, Murray BW, et al. IKK-1 and IKK-2: cytokine-activated IκB kinases essential for NF-κB activation. Science 1997;278:860–6.
20. Meier F, Schittek B, Busch S, et al. The RAS/RAF/MEK/ERK and PI3K/AKT signaling pathways present molecular targets for the effective treatment of advanced melanoma. Front Biosci 2005;10:2986–3001.
21. Hess AR, Hendrix MJ. Focal adhesion kinase signaling and the aggressive melanoma phenotype. Cell Cycle 2006;5:478–80.
22. Wellbrock C, Karasarides M, Marais R. The RAF proteins take centre stage. Nat Rev Mol Cell Biol 2004;5:875–85.
23. Pan WH, Devlin HF, Kelley C, Isom HC, Clawson GA. A selection system for identifying accessible sites in target RNAs. RNA 2001;7:610–21.
24. Yates J, Warren N, Reisman D, Sugden B. A *cis*-acting element from the Epstein-Barr viral genome that permits stable replication of recombinant plasmids in latently infected cells. Proc Natl Acad Sci U S A 1984;81:3806–10.
25. Kashani-Sabet M, Liu Y, Fong S, et al. Identification of gene function and functional pathways by systemic plasmid-based ribozyme targeting in adult mice. Proc Natl Acad Sci U S A 2002;99:3878–83.
26. Yang J, Fan GH, Wadzinski BE, Sakurai H, Richmond A. Protein phosphatase 2A interacts with and directly dephosphorylates RelA. J Biol Chem 2001;276:47828–33.
27. Ravi R, Bedi A. NF-κB in cancer—a friend turned foe. Drug Resist Updat 2004;7:53–67.
28. Monks NR, Biswas DK, Pardee AB. Blocking anti-apoptosis as a strategy for cancer chemotherapy: NF-κB as a target. J Cell Biochem 2004;92:646–50.
29. Ueda Y, Richmond A. NF-κB activation in melanoma. Pigment Cell Res 2006;19:112–24.
30. Hu Y, Baud V, Delhase M, et al. Abnormal morphogenesis but intact IKK activation in mice lacking the IKKα subunit of IκB kinase. Science 1999;284:316–20.
31. Li Q, Van Antwerp D, Mercurio F, Lee KF, Verma IM. Severe liver degeneration in mice lacking the IκB kinase 2 gene. Science 1999;284:321–5.
32. Stein CA. The experimental use of antisense oligonucleotides: a guide for the perplexed. J Clin Invest 2001;108:641–4.
33. Wellbrock C, Ogilvie L, Hedley D, et al. V599EB-RAF is an oncogene in melanocytes. Cancer Res 2004;64:2338–42.
34. Serrano M, Hannon GJ, Beach D. A new regulatory motif in cell-cycle control causing specific inhibition of cyclin D/CDK4. Nature 1993;366:704–7.
35. Greten FR, Eckmann L, Greten TF, et al. IKKβ links inflammation and tumorigenesis in a mouse model of colitis-associated cancer. Cell 2004;118:285–96.
36. Hanson JL, Hawke NA, Kashatus D, Baldwin AS. The nuclear factor κB subunits RelA/p65 and c-Rel potentiate but are not required for Ras-induced cellular transformation. Cancer Res 2004;64:7248–55.
37. Dajee M, Lazarov M, Zhang JY, et al. NF-κB blockade and oncogenic Ras trigger invasive human epidermal neoplasia. Nature 2003;421:639–43.
38. Zhang JY, Green CL, Tao S, Khavari PA. NF-κB RelA opposes epidermal proliferation driven by TNFR1 and JNK. Genes Dev 2004;18:17–22.
39. Baumgartner B, Weber M, Quirling M, et al. Increased IκB kinase activity is associated with activated NF-κB in acute myeloid blasts. Leukemia 2002;16:2062–71.
40. Karin M, Yamamoto Y, Wang QM. The IKK NF-κB system: a treasure trove for drug development. Nat Rev Drug Discov 2004;3:17–26.
41. Kim HJ, Hawke N, Baldwin AS. NF-κB and IKK as therapeutic targets in cancer. Cell Death Differ 2006;13:738–47.
42. Strieter RM. Mastering innate immunity. Nat Med 2003;9:512–3.
43. Pan WH, Xin P, Morrey JD, Clawson GA. A self-processing ribozyme cassette: utility against human papillomavirus 11 E6/E7 mRNA and hepatitis B virus. Mol Ther 2004;9:596–606.
44. Karin M, Cao Y, Greten FR, Li ZW. NF-κB in cancer: from innocent bystander to major culprit. Nat Rev Cancer 2002;2:301–10.

Systemic Targeting Inhibitor of κB Kinase Inhibits Melanoma Tumor Growth

Jinming Yang, Wei-Hua Pan, Gary A. Clawson, et al.

Cancer Res 2007;67:3127-3134.